Indices of Cardiorespiratory Synchronization from Rat Blood Pressure Data

N.B. Janson[1]*, N.B. Igosheva[2]†, A.G. Balanov[1],
O. Glushkovskaya-Semyachkina[2], T.G. Anishchenko[2], P.V.E. McClintock[1]

August 1, 2003

[1] Department of Physics, Lancaster University, Lancaster, LA1 4YB, UK
[2] Department of Biology, Saratov State University, Astrakhanskaya str. 83,
410026, Saratov, Russia

Abstract

A recently developed method for the detection of phase synchronization between several oscillatory processes from one-dimensional signals has been extended to allow estimation of synchronization indices. It has been applied to blood pressure signals from freely moving rats. Each rat underwent four stages: 1) healthy; 2) healthy but challenged by beta-blockers; 3) with stress-induced myocardial injuries; 4) with the stress-induced injuries challenged by beta-blockers. It is shown that cardiorespiratory synchronization plays an essential role at each of these stages.

1 Introduction

Synchronization is one of the most fundamental phenomena in the physics of oscillations. This effect can occur between self-sustained oscillators, i.e. in systems that are nonlinear, dissipative, and able to produce undamped oscillations, given an external energy supply. Note that the timescale of the oscillations is not equal to that of the energy supply (which would make the oscillations forced rather than self-sustained). The motion in such systems can be periodic, quasiperiodic, chaotic or induced by noise [1]. The oscillators can be coupled mutually or uni-directionally. In general, synchronization means the adjustment of basic oscillatory timescale(s) due to coupling. Several manifestations of this effect have been identified, and they may be substantially different in chaotic systems [2, 3, 4, 5, 6]. In systems whose dynamics is periodic albeit perhaps noise-influenced, however, the varieties of synchronization are reduced to frequency, or phase synchronization [7]. Phase synchronization seems to be the most general effect. It can arise in all known kinds of oscillating system. Introducing individual phases $\phi_i(t)$, $i = 1, 2$ for each pair of systems involved in interaction, we may consider the generalized phase difference $\Delta\phi(t)$, with due account of the inferred order of synchronization $n{:}m$, where n and m are integers [8]:

$$\Delta\phi(t) = \frac{n}{m}\phi_1(t) - \phi_2(t). \tag{1}$$

---

*n.janson@lancaster.ac.uk

†igosheva@chaos.ssu.runnet.ru

It is said that $n{:}m$ phase synchronization occurs if $\Delta\phi(t)$ has plateaus of sufficiently long duration. Phase synchronization between the main heart rhythm and spontaneous respiration in humans in the relaxed state was established in [9]. It has recently been shown that cardiorespiratory synchronization can serve as a diagnostic criterion in humans [10] and dogs [11], and that the order of synchronization can serve as a measure of depth of anaesthesia in rats [12].

A commonly used method for the detection of $n{:}m$ phase synchronization is to record signals from each of the interacting systems, compute phases from each signal, and then compare them using Eq. (1) [13]. This approach has been applied to the detection of cardiorespiratory synchronization [9, 12, 14]. However, it often happens that several processes with different timescales interact within a larger system, and that only a single signal is available at the output, e.g. only an electrocardiogram (ECG) without a respiration signal. Recently, a general approach was suggested for tackling such situations [15, 16, 17]. In this paper we apply it to the detection of phase synchronization, or its absence, between respiration and cardiac rhythm in rats, using the blood pressure signal alone. We extend the method reported previously in order to compute the synchronization index first introduced in [18]. We create an algorithm that allows us to find automatically the synchronization order $n{:}m$ for which the synchronization index is largest. By analysis of data from 7 male and 6 female rats, in four different states, we show that synchronization plays an essential role in cardiorespiratory interaction in rats, both in the healthy state and when under the influence of drugs or stress.

2   Experimental data

Experiments were performed on 13 adult Sprague-Dawley rats, 7 males and 6 females. Each animal was instrumented with an intra-arterial catheter for direct blood pressure recording. We note that in freely-moving rats it is difficult to make reliable measurements of respiration because the conventional transducers cannot safely be kept in the same position.

A series of experiments has been carried out in order to characterize blood pressure dynamics at rest, and also to observe slow transient processes induced by the intravenous injection of a nonselective beta-adrenoreceptors blocker, propranolol. All measurements were made on conscious, freely-moving, rats, and each animal underwent four stages of data acquisition:

   I "Healthy state" at rest (90 minutes)

  II "Healthy state", immediately after a propranolol injection (90 minutes)

 III "Unhealthy state", immediately after being subjected to stress that induced myocardial injuries (30 minutes)

 IV "Unhealthy state", immediately after propranolol injection, that was made 30 minutes after stress termination (90 minutes)

Stages (I) and (II) of the measurements took place one day after surgery to implant the catheter, with stages (III) and (IV) the following day after. By "healthy state" we mean the one with no sign of cardiovascular disease. By "unhealthy state" we denote significant but reversible structural and microcirculatory alterations in the myocardium, revealed by hystological analysis and resembling those observed at the initial stage of myocardial

ischemia. These injuries were induced by combination of immobilization and intermittent sound stimuli during two hours.

Injection of the beta-blocker propranolol (concentration 1mg/kg) simulated slow, monotonic, change in some internal parameters influencing the system. Namely, the concentration of beta-blocker in the blood influences the average heart rate and its dynamics in time. The rate of decrease of propranolol content in blood is much smaller than average heart rate, except for the very first minutes after injection. Its variation in time is known from pharmokinetics to be approximately exponential. Thus, by studying how the dynamics of cardiovascular system changes in time, we can to a certain extent study how it depends on the concentration of propranolol.

3 Detecting synchronization: finding the order $n{:}m$ and index

The blood pressure signals were typically of the shape shown in Fig. 1(a), and in more detail in (b). Here and in what follows values of the continuous blood pressure signal $x(t)$ and its local maxima x^{max} and minima x^{min} are given in mm of Hg. Typically, the Fourier spectrum of the blood pressure signal (Fig. 1 (c)) contains a sharp peak at the frequency of the average heart rate (AHR) f_{AHR}, a well-defined peak at the average respiration frequency f_{resp}, their combinations and, possibly, some lower-frequency components. We are interested in interactions between the cardiac and respiratory processes. To find out whether they are synchronous, or not, using just the blood-pressure signal, we exploit the approach recently developed in [15, 16] and applied to human heart rate variability data in [17, 19]. To quantify the degree of synchronization, if any, we extend this approach so as to be able to use synchronization index introduced in [18]. In this paper we describe the technical issues of the approach used, and for theoretical background refer the reader to [15, 16]. Data-processing took place in the following sequential stages –

1. Extracting discrete data. The first step is to extract from the continuous-time signal some discrete variables associated with a Poincaré map defined for the system under study. Typical discrete variables can be threshold-crossing interspike intervals, or return times T_i, which are the time intervals between successive crossings of the signal over some threshold level in one direction; successive local minima x_i^{min} or local maxima x_i^{max} (Fig. 1(b), Fig. 1(d)). The clinical significance of these variables is that: T_i are heart rate variability data; x_i^{min} is the diastolic, and x_i^{max} is the systolic, pressure during one heart beat. We can apply the approach developed to any kind of discrete data, but we note (see Fig. 1(b), Fig. 1(d)) that the amplitude variables x_i^{min} and x_i^{max} often display more stability compared to the temporal variable T_i. In this paper we will seek possible phase synchronization between heart rate and respiration through a study of x_i^{min}.

2. Filtering. Next, the low-frequency floating of average level from discrete data was reduced in order to concentrate on two higher-frequency processes: the main heart rhythm and respiration. We use two methods here. The first of these consists of computing the analogue of the second derivative of the original discrete time series $x(i)$:

$$x_{\text{der}}(i) = \frac{x(i+1) + x(i-1) - 2x(i)}{2}. \tag{2}$$

Let us refer to this method as to the *method of derivatives*. How it works as applied to x_i^{min} is illustrated in Fig. 2 (a), where the grey points indicate original data, and black ones those after filtration and addition of the average value x_{av}.

The second method is an extension of the well-known detrending technique. A local average is defined within a temporal window moving along the dataset, which is then subtracted from each datapoint. The only distinction of our method is that the size of the temporal window is not constant along the dataset. Namely, one window includes all points between two successive extrema (maximum and minimum, etc.) of a discrete signal, including extrema themselves. After the local average is computed within each window, its value is attributed to the time moment of window beginning. All such averages are then connected by straight lines by means of linear interpolation. Finally, from each original datapoint the value of the resultant graph is subtracted. In Fig. 3 (a) grey points show original data, the thin black line shows the local average, and black points show the filtered data, to which total average value x_{av} is added for the convenience of comparison.

3. Delay embedding is then applied, and the set of points is plotted in the plane x_{i+1} vs x_i. In Figs. 2 (b) and 3 (b) the delay plots are shown for the same dataset that had undergone two types of filtering. In both cases, three clouds of points can be observed in the phase portrait, hinting at 1:3 synchronization.

4. Extracting angles φ_i. On the delay plot (Figs. 2(b) and 3(b)) one defines an angle φ_i between each phase point and the abscissa axis. The resultant time dependences of angles are shown in Figs. 2(c) and 3(c). The plots of successive angle versus the previous one are given in Fig. 2(d) and 3(d). Here, the grey line shows the return function of the angles map derived in [15, 17]:

$$\phi_i = \arctan\left(2\cos 2\pi\xi - \cot\phi_{i-1}\right), \tag{3}$$

for the rotation number $\xi = n{:}m = 1{:}3$.

5. Transforming angles φ_i into relative phase Ψ_i. This stage is optional, but it can be used to ensure the rigour of the physical meaning of the obtained synchronization index. In [16] a relationship was established between angles φ_i of return times map or of the reconstructed Poincaré map, and the relative phase Ψ_i introduced in [13]:

$$\tan\varphi_i = \frac{\cos\left(\Psi_i + \frac{3\Theta}{2}\right)}{\cos\left(\Psi_i + \frac{\Theta}{2}\right)} = \cos\Theta - \tan\left(\Psi_i + \frac{\Theta}{2}\right)\sin\Theta, \quad \Theta = 2\pi\xi, \tag{4}$$

where ξ is rotation number. Note, that Eq. (4) is valid only if the coupling between the processes under study can be treated as vanishingly small. Knowledge of φ_i allows one to use Eq. (4) to extract relative phase Ψ_i, provided that the rotation number ξ, equal to $n{:}m$ in the case of synchronization, is known. Thus, one should find the suspected order of synchronization $n{:}m$. This can be done e.g. by computing the Fourier spectrum for the given sample of data and locating the highest peaks, namely, presumed to be those derived from heart rate and respiration, as in Fig. 1(c). The closest rational approximation to the ratio f_{resp}/f_{AHR} can provide one with a guess at the suspected synchronization order $n{:}m$. Note that Eq. (4) cannot be used for $\xi = 1:2$ because the latter produces a singularity. Fig. 4(a) shows the angles φ_i that are transformed into the relative phase Ψ_i, which is shown in Fig. 4(b), with $\xi = 1:3$.

6. Unwrapping the relative phase or angles to obtain $n{:}m$ phase difference. The angles φ_i, or relative phase Ψ_i, fall by construction in the range $[-\pi; \pi]$. We need to unwrap these variables into the natural interval $]-\infty; \infty[$ in order to obtain the conventional phase difference at the time moment t_i to which the original discrete variable like x^{min} is attributed. The proposed algorithm is as follows. We introduce an integer k, starting with $k=0$, that increases (decreases) by 1 with each phase jump in negative (positive) direction. To detect a phase jump, we consider two consecutive values, say Ψ_{i-1}

and Ψ_i, and at each step i estimate the difference between them. If the absolute value of this difference is larger than $\pi/2$, this counts as a phase jump and the value of k is adjusted accordingly. The unwrapped variable is set to be $\Psi_i^u = \Psi_i + 2\pi k$. In Fig. 4(c) the 1:3 phase difference is shown that was obtained from relative phase in Fig. 4(b).

7. Transforming the n:m phase difference into a 1:1 phase difference by setting $\Psi_i^{1:1} = \Psi_i^u * m - 2\pi i$.

8. Wrapping of 1:1 phase difference into the interval $[-\pi; \ \pi]$ can easily be effected by repeatedly subtracting 2π from each value of $\Psi_i^{1:1}$, until the latter falls within the required interval. Fig. 4(d) illustrates this final stage of data transformation and shows the 1:1 phase difference wrapped into the interval $[-\pi; \ \pi]$.

9. Computation of synchronization index, by application of the algorithm introduced in [18] to the value of $\Psi_i^{1:1}$. We introduce a temporal window of length L and move it along the data in steps of a chosen size. Inside the window, for its starting point number i, the value of ρ is estimated as:

$$
\begin{aligned}
\rho_c &= \frac{1}{L} \sum_{j=1}^{L} \cos \Psi_{i+j-1}^{1:1} \\
\rho_s &= \frac{1}{L} \sum_{j=1}^{L} \sin \Psi_{i+j-1}^{1:1}, \quad \rho = \sqrt{(\rho_c^2 + \rho_s^2)},
\end{aligned}
\tag{5}
$$

ρ being the index of synchronization sought. It is obvious that ρ can vary between 0 and 1, the former meaning absence of synchronization, the latter perfect synchronization, and values in between implying various intermediate degrees of synchronization. For the noisy processes that we deal with in real life ρ can never reach 1.

Note, that stages (5)-(7) require a reliable estimate of the synchronization order n:m. One usually wants to make computations automatically, but a proper guess of n:m often requires some manual selection of spectral peaks (although this could also be rendered automatic in principle). To simplify the situation, we form a set of most frequently encountered synchronization orders with reasonably small numerators and denominators, and repeat stages (5)-(7) for all of them. We thus obtain a synchronization index for each synchronization order from each data set.

4 Synchronization indices for rat data

A set of the following rotation numbers was tried for each blood pressure signal:

$$
\xi_j: \quad 1:2, \quad 1:3, \quad 1:4, \quad 1:5, \quad 1:6, \quad 2:5
\tag{6}
$$

The above numbers are rational approximations of the most frequent ratios of respiration frequency f_{resp} to average heart rate f_{AHR} estimated from Fourier spectra of the blood pressure signal. A temporal window of length $L = 500$ was selected by trial and error. It is small enough to reflect a ρ close to instantaneous one, and large enough to provide good averaging for ρ. ρ_j was estimated within one window for all ξ_j indicated in Eq. (6), and the largest ρ^{max} was selected.

In Figs. 5, 6, 7, 8 the horizontal axis is equivalent time. Each different shade marks a different stage of the experiment, the data for each stage (I), (II), (III) and (IV) being placed sequentially. For additional clarity, the different stages are separated by vertical dashed lines. Note, that the time is in fact not continuous here, since there could be substantial time gap between stages (I) and (II), (II) and (III). The letters "f" and "m"

to the right of the plots denote female or male rats respectively, and the numbers label different animals.

In Figs. 5 and 6 the largest synchronization indices ρ^{max} are shown for each rat dataset. In Figs. 7 and 8 the rotation numbers corresponding to the ρ^{max} are given. One can see that the synchronization index is generally small, indicating a low degree of synchronism between heart rate and respiration in rats. An interesting observation is that in conscious freely-moving rats 1:2 synchronization is quite often encountered in the states considered, contrary to observations made on humans, for which such a regime is very unnatural. Namely, at stage (I) order 1:2 prevailed in 5 of 7 male rats, and in 3 of 6 female rats.

In 7 of the 13 animals (4 female and 3 male), development of stress-induced myocardium alterations was accompanied by a decrease in synchronization index. Propranolol administered after stress restored the synchronization index to basal values in female rats, but not in the males.

It should be noted that although in most rats stress-induced alterations in the myocardium were reversible, there were three animals in which stress induced irreversible injuries resulting in a near-death state: those marked "f2", "f5" and "m1". In these animals stress caused the synchronization order to be 1:2 most of the time; injection of propranolol that was intended to cure them in a certain sense, did not change it. In contrast, for female rats the synchronization index was markedly increased.

5 Conclusions

A method for detecting phase synchronization from one-dimensional data was applied to the blood pressure signals of conscious freely-moving rats in different states. It allowed us to detect the presence or absence of synchronization between the cardiac and respiratory processes. The method was further developed in order to automatically estimate the synchronization index from the experimental data.

13 animals of both genders were studied, in each of four different states, in order to reveal how the order and strength of cardiorespiratory synchronization are dependant on the state of cardiovascular system. There were two steady states: "healthy" and "unhealthy", and two long slow transient processes induced by injection of a beta-blocker into a rat in each of these basic states. It was found out that, in common with humans, cardiorespiratory synchronization in rats is generally not very strong. However, the typical synchronization orders seem to be higher than in humans. In particular, 1:2 synchronization – which is untypical in healthy humans at rest – was often encountered in conscious rats at all stages including rest. It seems that no unique response to stress and/or drugs could be revealed in rats in terms either of the order $n{:}m$, or of the index ρ of carioresipratory synchronization. Rather, each animal responded individually to external influence.

6 Acknowledgements

References

[1] H. Gang, T. Ditzinger, C.N. Ning & H. Haken, "Stochastic resonance without external periodic force", *Phys. Rev. Lett.* **71**, 807-810 (1993).

[2] H. Fujisaka, Y. Yamada, "Stability theory of synchronized motion in coupled-oscillator systems", *Progr. Theor. Phys.* **69**, 32 (1983).

[3] M.G. Rosenblum, A.S. Pikovsky, and J. Kurths, "From phase to lag synchronization in coupled chaotic oscillators", *Phys. Rev. Lett.* **78**, 4193 (1997).

[4] N.F. Rulkov, M. Sushchik, L.S. Tsimring, and H.D.I. Abarbanel, "Generalized synchronization of chaos in directionally coupled chaotic systems", *Phys. Rev. E* **51**, 980 (1995).

[5] V.S. Anishchenko, T.E. Vadivasova, D.E. Postnov, M.A. Safonova, "Forced and mutual synchronization of chaos", *Radiotehn. Elektron (Moscow)* **36**, 338 (1991).

[6] M. Rosenblum, A. Pikovsky, J. Kurths, *Phys. Rev. Lett.* "Phase synchronization of chaotic oscillators", **76**, 1804 (1996).

[7] R.L. Stratonovich, "Topics in the theory of random noise", (Gordon & Breach), 1963.

[8] A. Pikovsky, M. Rosenblum and J.Kurths, "Synchronization. A Universal Concept in Nonlinear Science", Cambridge University press (2001)

[9] C. Schäfer, M.G. Rosenblum, J. Kurths, H.H. Abel, "Heartbeat synchronized with ventilation", *Nature* **392**, 239 (1998).

[10] R. Mrowka, A. Patzak, and M.G. Rosenblum, "Quantitative analysis of cardiorespiratory synchronization in infants", *Int. J. of Bifurcation and Chaos* **10**(11), 2479 (2000).

[11] H. Seidel, H. Herzel, "Bifurcations in a nonlinear model of the baroreceptor-cardiac reflex", *Physica D* **115**, 145 (1998).

[12] A. Stefanovska, H. Haken, P.V.E. McClintock, M. Hožič, F. Bajrovič, and S. Ribarič, "Reversible transitions between synchronization states of the cardiorespiratory system" *Phys. Rev. Lett.* **85**, 4831 (2000).

[13] C. Schäfer, M.G. Rosenblum, H.-H. Abel, J. Kurths, "Synchronization in the human cardiorespiratory system", *Phys. Rev. E* **60** (1), 857-870 (1999).

[14] S. Rzeczinski, N.B. Janson, A.G. Balanov, P.V.E. McClintock, "Regions of cardiorespiratory synchronization in humans under paced respiration", *Phys. Rev. E* **66**, 051909 (2002).

[15] N.B. Janson, A.G. Balanov, V.S. Anishchenko, and P.V.E. McClintock, "Phase synchronization between several interacting processes from univariate data" *Phys. Rev. Lett.* **86**, 1749 (2001).

[16] N.B. Janson, A.G. Balanov, V.S. Anishchenko, and P.V.E. McClintock, "Phase relationships between two or more interacting processes from one-dimensional time series. I. Basic theory", *Phys. Rev. E* **65**, 036211 (2002).

[17] N.B. Janson, A.G. Balanov, V.S. Anishchenko, and P.V.E. McClintock, "Phase relationships between two or more interacting processes from one-dimensional time series. II. Application to heart-rate-variability data", *Phys. Rev. E* **65**, 036212 (2002).

[18] P. Tass, M.G. Rosenblum, J.Weule, J. Kurths, A.S. Pikovsky, J.Volkmann, A.Schnitzler, and H.-J.Freund "Detection of n:m phase locking from noisy data: application to magnetoencephalography", *Phys. Rev. Lett.* **81**, 3291 (1998).

[19] N.B. Janson, A.G. Balanov, V.S. Anishchenko, and P.V.E. McClintock, "Modelling the dynamics of angles of human R-R intervals", *Physiol. Meas.* **22**, 565 (2001).
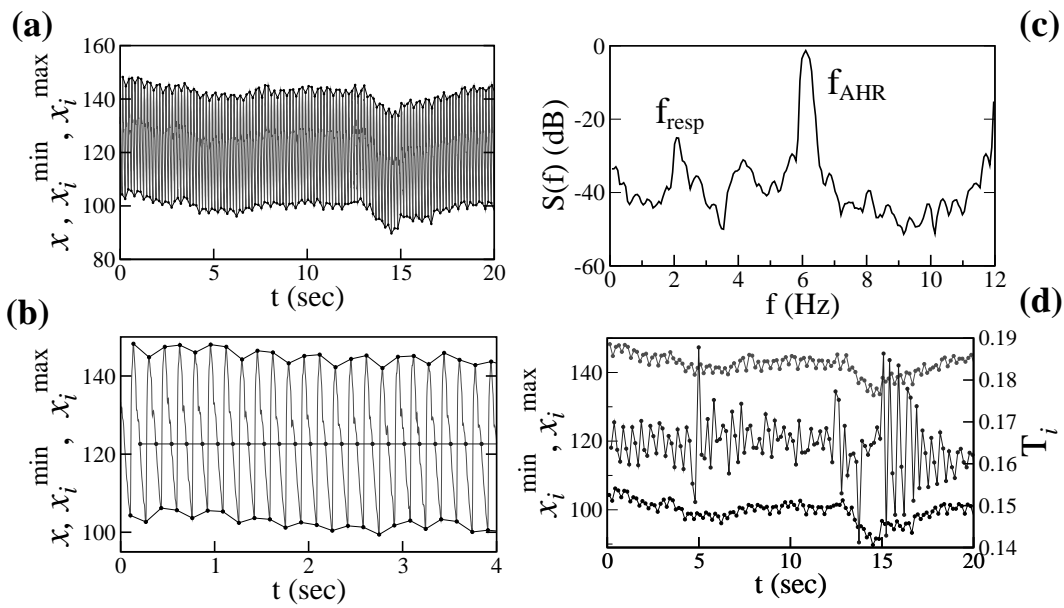
Figure 1: (a), (b) Blood pressure signal of a rat in mmHg. Filled circles show the positions of extrema which are instantaneous systolic (maxima) and diastolic (minima) pressures. (a) Interval 20 sec (b) Interval 4 sec. (c) Fourier power spectrum of signal shown. f_{AHR} and f_{resp} are average heart rate and respiration frequency, respectively. (d) Discrete variables extracted from signal shown in (a): x_i^{min} (lower curve), x_i^{max} (upper curve), both in mmHg; T_i in seconds (middle curve).
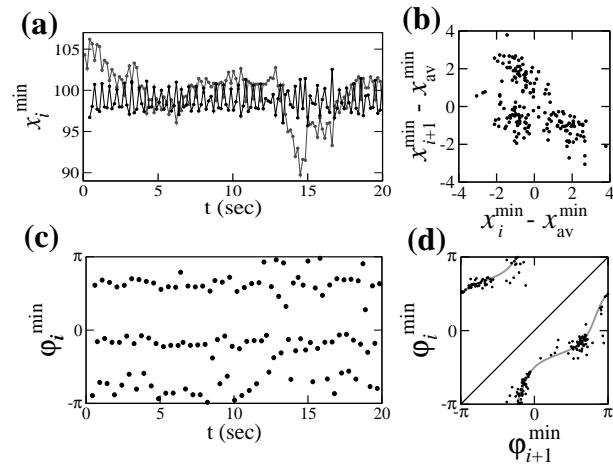
Figure 2: Illustration of the first filtering technique: derivatives method. (a) Position of original minima x_{min} (grey) and filtered data with added average value (black); (b) map of filtered x_{min}; (c) angles of the map in (b) versus time; (d) map of angles. Grey line in (d) shows the return function of map (3) for $\xi = 1/3$.
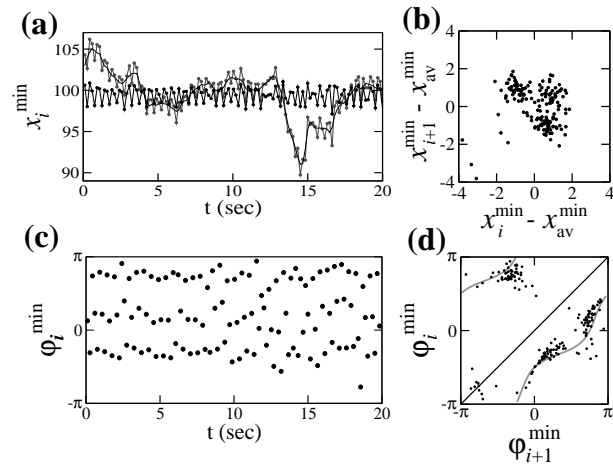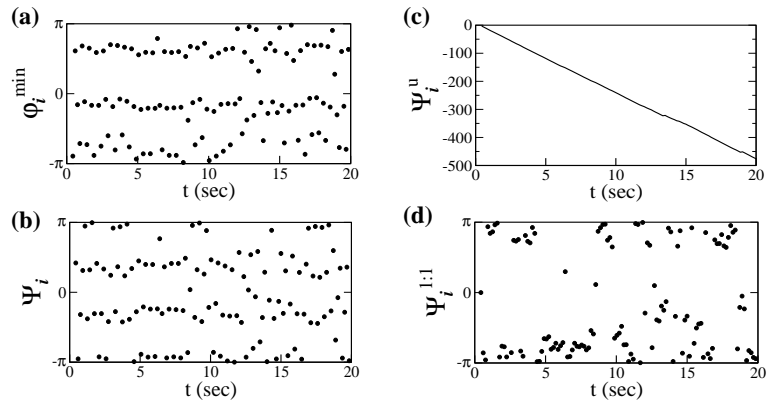
Figure 3: Illustration of the second filtering technique: differences method. (a) Position of original minima x_{min} (grey) and filtered data with added average value (black); (b) map of filtered x_{min}; (c) angles of the map in (b) versus time; (d) map of angles. Grey line in (d) shows the return function of map (3) for $\xi = 1/3$.

Figure 4: Illustration of how the angles φ_i are transformed into the form suitable for computation of synchronization index. (a) angles φ_i of map of x^{min} filtered by derivatives (the same as Fig. 2(c)); (b) relative phase Ψ_i reconstructed from angles by means of Eq. (4); (c) unwrapped relative phase Ψ_i^u; (d) phase difference $\Psi_i^{1:1}$ wrapped into $[-\pi;\ \pi]$.
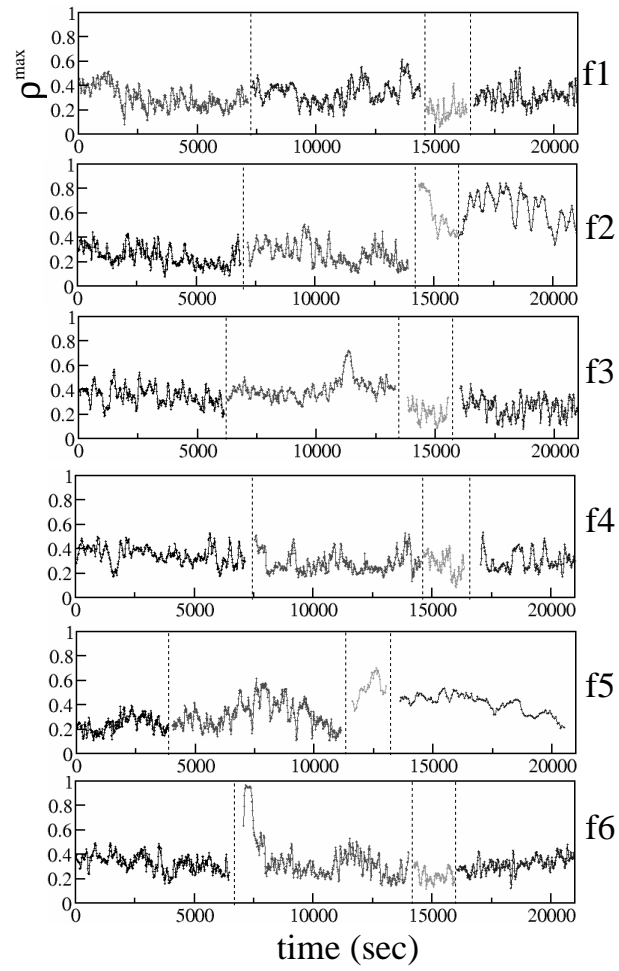
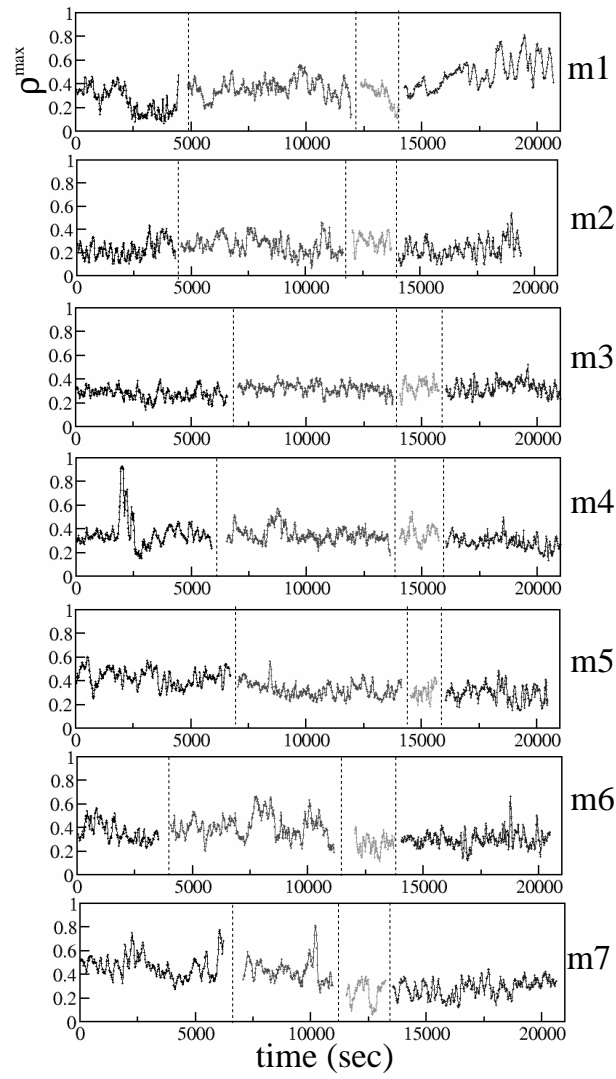Figure 5: Largest synchronization index versus time for female rats. Details in text.

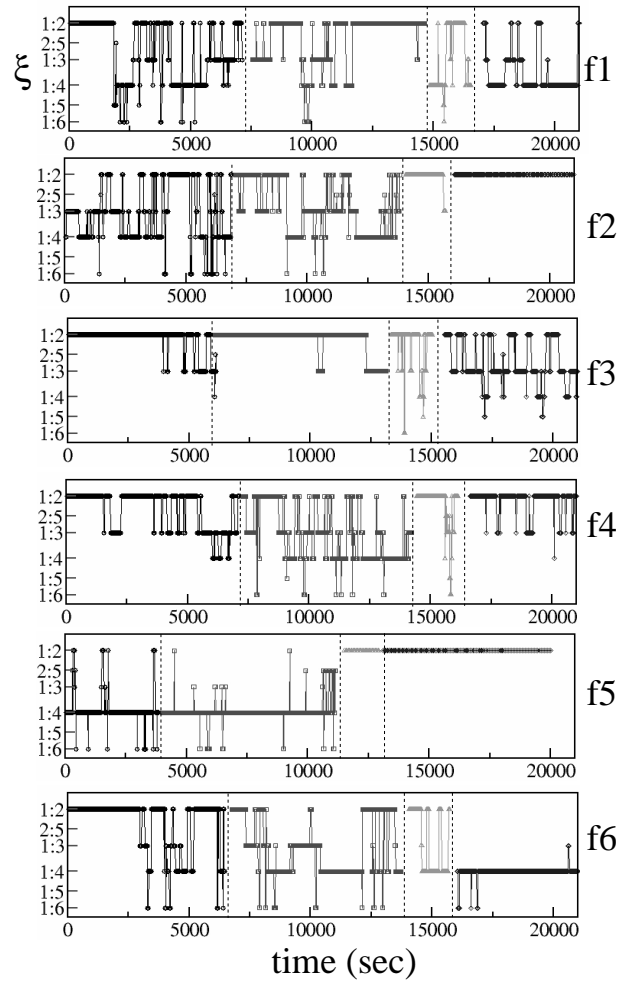Figure 6: Largest synchronization index versus time for male rats. Details in text.

Figure 7: Rotation number for largest synchronization index versus time for female rats. Vertical axis is in logarithmic scale. Details in text.
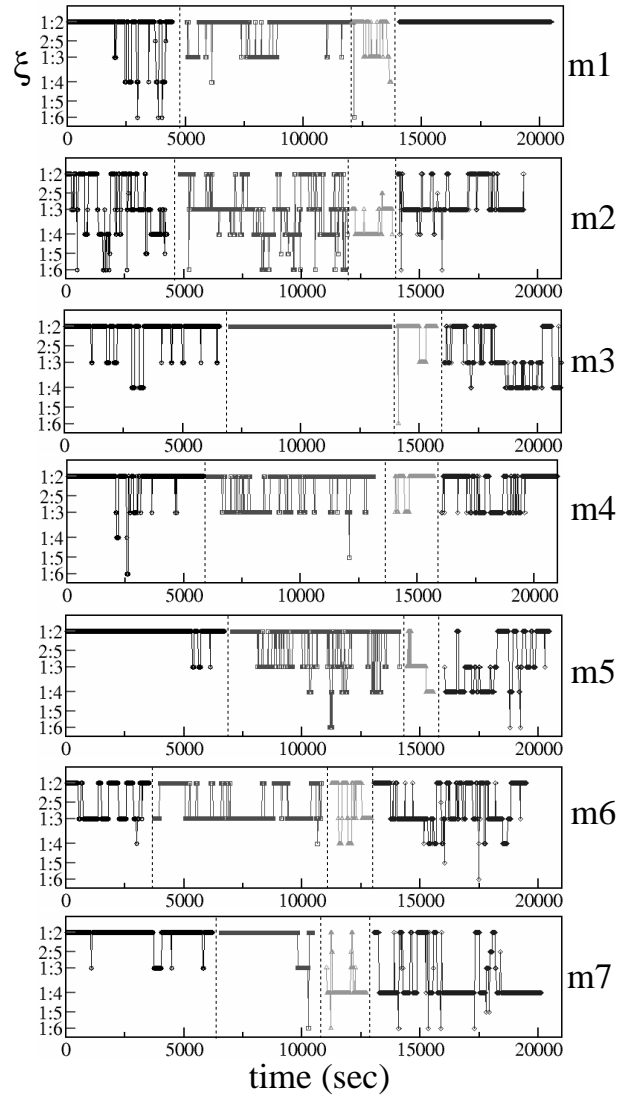
Figure 8: Rotation number for largest synchronization index versus time for male rats. Vertical axis is in logarithmic scale. Details in text.